energies

MDPI

Article

Heat Transfer and Energy Consumption of Passive House in a Severely Cold Area: Simulation Analyses

Fang Wang [1], Wen-Jia Yang [1] and Wei-Feng Sun [2,*]

[1] School of Mechanical and Power Engineering, Rongcheng College, Harbin University of Science and Technology, Harbin 150080, China; wangfang0228@hrbust.edu.cn (F.W.); wenjia_yang@126.com (W.-J.Y.)
[2] School of Electrical and Electronic Engineering, Harbin University of Science and Technology, Harbin 150080, China
* Correspondence: sunweifeng@hrbust.edu.cn; Tel.: +86-1584-659-2798

Received: 31 December 2019; Accepted: 30 January 2020; Published: 2 February 2020

Abstract: In order to improve the heat transfer in enclosure structure of passive houses in cold area with complex climatic conditions, a three-dimensional model is established to investigate the time-by-case changes of outdoor temperature and solar irradiation based on the principle of integral change and the method of response coefficient and harmonious wave reaction. The variations of hourly cooling and heating loads with outdoor temperature and solar irradiation are analyzed. As simulated by cloud computing technology, the passive building energy consumption meets the requirements of passive building specifications. In the present research, super-thermal insulation external wall, enclosure structure of energy-conserving doors and windows, and high efficiency heat recovery system are employed to achieve a constant temperature without active mechanical heating and cooling, which suggests a strategic routine to remarkably decrease the total energy consumption and annual operation cost of passive building.

Keywords: passive house; enclosure structure; heat transfer coefficient; energy consumption

1. Introduction

As the earth's temperature is increased by human energy consumption, great attention has been focused on high-comfort green buildings with renewable energy and near zero energy consumption, which are named "passive houses" and limit the sum of primary energy consumption to less than 120 kWh/(m^2·a). Early in 2005, Feist suggested the characteristics of combined heating and ventilation system in passive houses by investigating the energy consumption level and comfort index [1]. Passive housing and its standard were firstly proposed in Germany. After a long period of technical improvement, the standard required for passive houses gradually became more detailed and rigorous. In 2006, Schnieders tested eleven passive houses in Germany and concluded that passive houses can save 80% of space energy consumption, with the total primary energy consumption (including household electricity) being controlled lower than 50% of the traditional new buildings [2]. Based on the thermal performance of passive houses with arch roof in New Delhi, India, it is concluded by Arvind that the annual energy consumption of heating and cooling can be saved by 1481 kWh/a and 1814 kWh/a, respectively, with only 52 euros per year in carbon emission cost [3]. In 2011, Mlakar discussed the effects of different energy gains on the overheating in hot summer for a passive house in Slovenia compared with the actual heat consumption of traditional houses [4]. The construction standard of passive houses was firstly proposed by Rongen in 2012, which has become a globally recognized energy-saving building standard [5]. In 2013, Ridley reported that the total energy consumption of the first new London house certified by passive housing standard has approached to 65 kWh/(m^2·a), which is one of the lowest energy consumption for small family houses in UK [6].

Taking energy transportation cost into account and analyzing the energy consumption through the whole operation cycle, the per capita energy consumption of a typical passive house in Belgium is 19.6% lower than that of the traditional buildings before reconstructions [7,8]. Rohdin confirmed that the indoor comfort of nine passive houses in Sweden is better than that of traditional buildings without considering external shading, despite of the distinctly changed indoor temperature in summer due to cooking or other heat sources [9]. Irulegi was the first to study industrialized solar houses in which the architectural design strategy combined solar energy technology with passive design standards to achieve energy self-sufficiency and provide a high quality of life for occupants [10]. In 2016, Dan built an energy-saving house in Romania according to the design principles of passive house and proved that the total primary energy demand is less than the design goal of 120 kWh/(m^2·a) [11]. In 2019, Ilomets analyzed the indoor climate loads for dwellings in different cold climates to assess hygrothermal performance of building envelopes and put forward the suggestions for the external wall insulation [12].

The first passive house under subtropical climate in Cyprus was designed by Fokaides employing an optimized night ventilation equipment and a high efficient HVAC cooling system to reduce the average indoor temperature and significantly improve the thermal comfort, respectively [13]. A passive house in the Qivli District of Australia, which is designed using solar energy, heat, and transverse ventilation, represents a total energy consumption of 64% lower than similar households in the same city and provides excellent indoor comfort and a high air quality levels [14]. Alajmi studies the terminal energy consumption performance of double-decker villas built according to the passive house standards in Portland, Oregon, USA [15]. It is proved that passive houses achieve net zero energy consumption by using photovoltaic panels, which are suitable for the climate of northwest United States. The excellent structure, amenity, and power balance can be acquired by solar passive houses that adopt the solar energy and heating ventilation of air conditioning system as an efficient strategy to combine passive, active, and prefabricated systems [16]. Dalbem determines the thermal enclosure structure of different climates in southern Brazil according to the implementation standards of Brazilian passive houses and discusses the transformation of traditional houses into standard passive houses [17]. According to the standard of passive houses, the best scheme of Brazilian passive house has been obtained by analyzing the thermal performance index and economic feasibility with the optimized numerical model [17]. In southern Germany, the energy saving performance and CO_2 emissions of a newly built passive school implied that the passive houses have been extended to public buildings [18]. The latest version of the passive house standard was revised with new standard provisions in 2016 to be applied for all climates in the world, abating the restrictions on sub-cold and temperate climates and integrating the requirements for residential and non-residential buildings. The new standard requires that the heating or cooling demand of a passive house should be not higher than 15 kW·h/(m^2·a), the air tightness parameter should be no larger than 0.6 h^{-1}, the renewable energy demand should be no greater than 60 ± 15 kW·h/(m^2·a).

The energy saving rates of passive houses are much higher than that of traditional buildings; thus, it is of great significance to study and develop passive houses for the sustainable development of China where building energy consumption accounts for 1/3 of total energy consumption. In 2010, China built the first certified passive house of China—Hamburg House was built in Shanghai Expo Park [19]. In 2014, the first high-rise passive building in the area with hot summer and cold winter was built in Zhuzhou, Hunan Province of China [20]; and the first cold region passive house, Chenweili Bay, was built in Yingkou, Liaoning Province of China [21,22]. In 2015, the China passive Ultra-Low Energy Consumption Building Alliance organized for the China Academy of Architectural Sciences and other units to compile and issue the *Passive Ultra-Low Energy Consumption Green Building Technical Guidelines (Residential Buildings)* as the technical standard of passive houses in China [23]. According to China's sustainable development strategy, passive buildings with high energy efficiency and comfortable living are the prospective candidates for saving energy and reducing carbon emissions in the future in order to deal with climate change. By the end of 2018, more than 100 passive construction projects have

been accomplished in China, 21 of which have been certified as passive houses. However, due to the vast territory, large climatic coverage, and different complexity of climatic conditions in China, passive constructions are mainly concentrated in the southern regions while the passive projects in severely cold areas are less than 10% of total passive houses. Therefore, the present study takes Senying passive office building in Harbin city of China (a typical severely cold area) as a representative to carry out theoretical investigation and practical analysis, in order to conclude the heat transfer and energy consumption of passive house with enclosure structure that are suitable for a severely cold area, and provide fundamental reference for the design and construction of passive house in a severely cold area.

2. Simulation and Analysis Methodology

2.1. Passive House Standard

The passive house requires adaptation to climate characteristics and site conditions so that the energy consumption of heating, air conditioning, and lighting can be minimized through passive architectural design. In order to improve the efficiency of energy preservation equipment and systems, renewable energy is used in all areas to provide a comfortable indoor environment with minimal energy consumption. The indoor environmental parameters and energy efficiency indexes of passive houses must conform to standards so the energy consumption without using mechanical heating and cooling is reduced to a certain level under the premise of ensuring human body comfort. In recent years, passive building standards in China have been studied and explored in a deep way. In 2019, the Heilongjiang Provincial CPC Committee published the *Passive Low Energy Consumption Residential Building Design Standard* as listed Table 1 for the relevant design standards of passive house [24]. The space heating load of passive buildings in winter should not be greater than 12 W/m^2; the cooling load in summer should be less than 20 W/m^2, and the primary energy demand (including heating, cooling, domestic hot water, and living electricity) should be less than 120 kWh/m^2 per year. The heat transfer coefficients of enclosure structure and window for passive house must be lower than 0.1 and 0.8 W/(m^2·K) respectively, with the air tightness being controlled to a ventilation number of <0.5/h under the pressure difference of 50 Pa. In summary, the enclosure structure of passive building should possess excellent heat preservation and absolute tightness while the heat recovery system has sufficient recovery rate, which can sustain high air quality without window opening in winter and summer.

Table 1. Designing standards of passive house.

Parameter	Unit	Maximum
Heating demand	kWh/m^2	18
Heating load	W/m^2	12
Cooling demand	kWh/m^2	13
Cooling load	W/m^2	20
Frequency of overheating	%	10
Air tightness (n50)	ACH	0.6
Primary energy demand	kWh/m^2	120

2.2. Climatic and Geographical Characteristics and Building Data

Harbin city is located in the south of Heilongjiang Province of Northeast China Plain, between longitude 125°42′~140°10′ east and latitude 44°04′~46°40′ north. Harbin is the capital city with the highest latitude and the lowest temperature in China with the middle temperate continental monsoon climate as: distinct four seasons, long and cold winter, and short and cool summer. The temperature in Harbin changes rapidly in the transitional seasons of spring and autumn with relatively short time. Therefore, the thermal design area of Harbin is located in the severely cold region where the annual average temperature is 4.5 °C; the lowest temperature appears in January and can reach −40 °C; the indoor heating temperature is controlled at 18–22 °C, and the average heating time is 174 days.

The Senying passive office building studied in the present paper is a double-decker structure with a building height of 9 m and a total building area of 5025.74 m^2. The first-floor area is 2683.58 m^2 and the second-floor area is 2464.37 m^2, as the photographs and ichnography shown in Figure 1, and the side view schematics shown in Figure 2. The whole building utilizes super heat preservation honeycomb wall, being equipped with special passive doors and windows, sunshade shutters, photovoltaic power generation, rainwater collection, reclaimed water treatment, waste biochemistry, waste heat exchange, and sunshine utilization. The air tightness parameter (ACH at 50 Pa) of this passive house is only 0.16/h, which is far below the international standard of 0.6/h, and the annual total saving cost of heating and cooling approaches to 1.8 million ¥ with the annual total carbon dioxide emission being reduced by 4.2×10^5 kg.

Figure 1. Senying passive office building: close and panoramic photographs (upper and middle panels), and ichnography of the first floor (bottom panel).

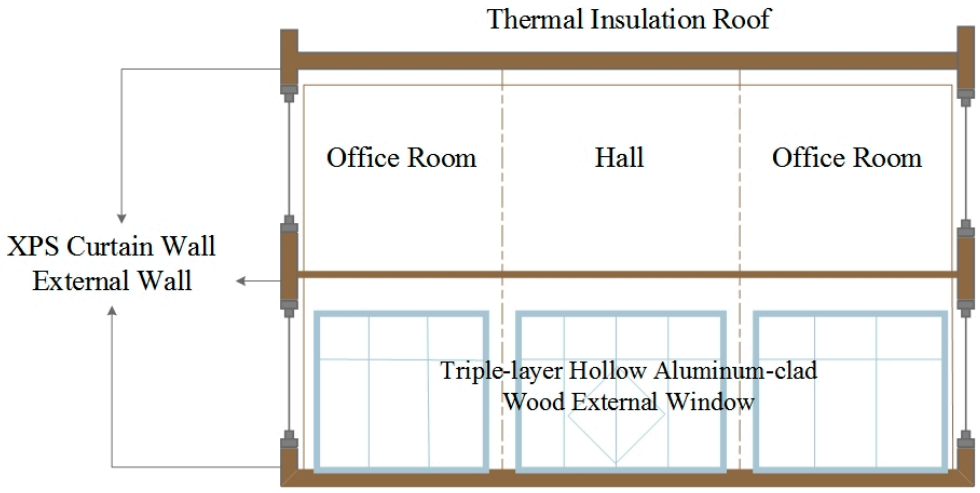

Figure 2. Side view of Senying passive office building.

2.3. Simulation Schemes and Design Parameters

The main factors of building energy consumption—envelope structure and ventilation efficiency—in the design strategy of passive buildings in a severely cold area are firstly determined to establish the building model and confirm the passive house design parameters. Then, the harmonic response method is used to calculate the thermal loads and heat transfer of wall roof, exterior window, and indoor with the various heat sources being divided into convection and radiation parts. By means of harmonic response method, the cooling load caused by the exothermic decay and delay between the different enclosure structures is specially evaluated in the radiation heat calculations, and the heat transfer caused by air penetration is included in the convection to calculate the total load. Finally, the relevant thermal loads and energy consumption are estimated and analyzed. The investigation strategy and simulation routine in the present study are schematically illustrated in Figure 3.

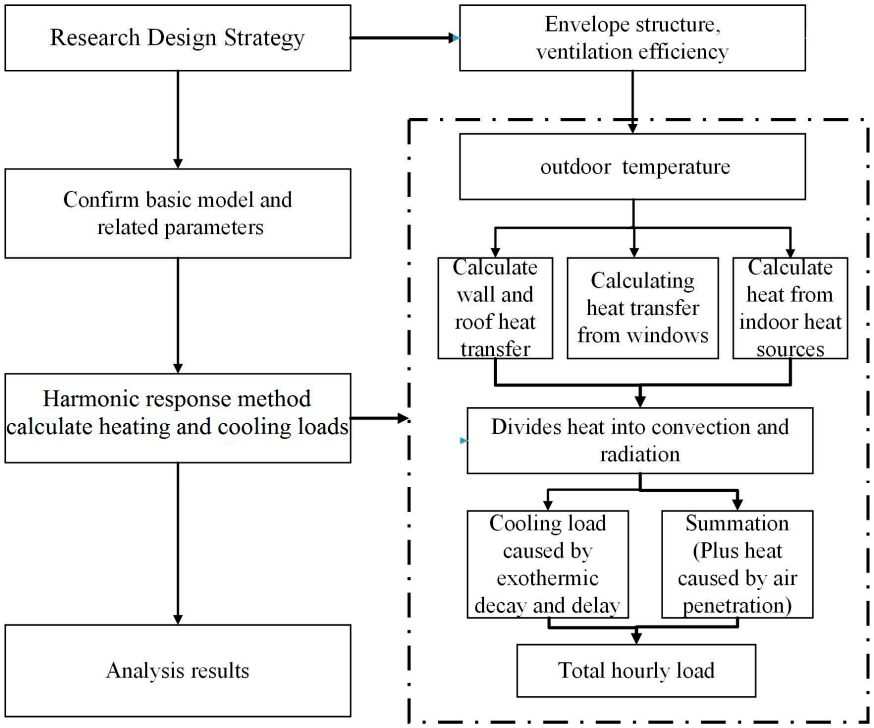

Figure 3. Schematic investigation strategy in simulation processes.

Taking Senying office building under the climate of Harbin as a paradigm, the three-dimensional model of passive house with spatial zoning and spatial tagging is established by the relevant design parameters of heat transfer environment and enclosure structure as shown in Tables 2 and 3, respectively. According to the thermal balance principle of heat transfer theory, the influences of heat transfer coefficient and thickness of different thermal insulation materials on the heat transfer performance of passive house enclosure structure are calculated and analyzed with the different structural combinations being compared. Based on the principle of integral variation, the Ecotect software is implemented to simulate the outdoor time-by-case temperature and variation of solar irradiation through a day. Employing the harmonic response method as implemented in BIM code, the hourly thermal load on the enclosure structure of passive house, which varies with outdoor temperature and solar irradiation is calculated and analyzed in the present study. Using cloud computing technology as implemented by the program Green Building Studio, we also perform energy cost analyses for the latent heat, energy, and carbon demand of passive house in severely cold area.

Table 2. Design parameters of heat transfer environment.

Summer mean temperature/°C		25
Winter mean temperature/°C		20
Outdoor mean temperature through a year/°C		4.5
Summer outdoor dry ball mean temperature/°C		30.6
Winter outdoor dry ball mean temperature/°C		−24.1
Outdoor mean air flow rate/(m/s)	Summer	2.8
	Winter	3.5
Relative humidity/%		60
Equipment power/(W/m^2)		13
Light power/(W/m^2)		11
Fresh air volume/(m^3/h)		60

Table 3. Envelope structure parameters.

Envelope Constitutes	Maximum Heat Transfer Coefficient/(W·m^{-2}·K^{-1})	Envelope Delay/h	Envelope Attenuation/%
Thermal insulation wall	0.125	13.3	4
Outside window	0.65	2.5	89
Floor	0.125	11.7	2
Roof	0.125	19.7	6
Interior wall	0.1	7.0	55
Exterior door	0.65	0.6	99

Ecotect and BIM are commonly used simulation software to analyze the energy consumption and heat transfer of buildings at present. With friendly user interface, high computational compatibility, and intuitive results, Ecotect and BIM are suitable for the analysis and research of meteorological data and building environment to provide the basis for the optimization and promotion of architectural design scheme, which is beneficial to the realization of an efficient architectural scheme design [25,26]. Using harmonic response method as being implemented by BIM to calculate the thermal loads has the advantages of simple calculation and no need for repeated iteration to be effectively applied in predicting the actual engineering energy consumption [26]. By harmonic response method, the attenuation and delay of the building enclosure structure can be considered to calculate the time-by-time load and energy consumption through a year.

3. External Enclosure Structure

3.1. Thermal Insulation System of External Wall

In order to realize a passive building, a certain thickness of high-efficiency thermal insulation materials, special passive doors and windows, mechanical ventilation equipment for heat recovery, and air tightness control are inbuilt, as shown in the schematic passive house structure in Figure 4. The enclosure structure is the main constituent, being directly in contact with the external environment and thereby acting as the dominant medium through which heat transfer and energy move between the inside and outside of passive building. In the enclosure structure, the external wall as the primary constituent contributes to the major area and contacts all the other parts of thermal maintenance system. In the whole building energy consumption, the external wall accounts for >40%, so the external wall design for thermal insulation is of great significance to the enclosure structure of passive house. The external insulation structure, as a structural complex to effectively reduce the energy consumption, is set up to connect with walls through an appropriate way in the enclosure structure. The external insulation medium mainly consists of special materials with obvious capability for heat insulation, heat preservation, and energy saving. According to the practical construction features, the external wall insulation can be classified into three forms: interior thermal insulation, exterior insulation, and sandwich insulation [27], as shown in Table 4 which provides the advantages and disadvantages of three different thermal insulation structures.

In comparison for these three thermal insulation forms, the interior heat preservation occupies a larger space and lacks structural protection, and the sandwich insulation is not technologically mature and has higher construction costs, while the exterior insulation is simple in structure and easy to manufacture with developed processing technology. Therefore, considering the practical situation in Harbin, we adopt the exterior insulation system for the external wall structure of passive house to meet the standard of ultra-low energy consumption. Further, passive buildings are simultaneously required to comply with fire prevention specifications. At present, the primary four kinds of thermal insulation materials applied for passive external walls are classified as follows [28]: (1) Graphite-Molded Expanded Polystyrene Sheet (GEPS), fabricated by adding graphite particles and infrared reflector agents in the production of normal Expanded Polystyrene Sheet (EPS), which presents low thermal conductivity and high flame retardancy; (2) Extruded Foam Polystyrene Sheet (EFPS), which is obtained by uniformly extruding the molten polystyrene and appropriate additives from a pressing extruder, has smooth surfaces without pores, high tenacity, low hydrophilicity, and excellent heat preservation performance; (3) Polyurethane Foam Board (PUFB) with a small heat transfer coefficient can effectively reduce the wall thickness but at high cost; (4) Stone Wool Board (SWB) is an inorganic material with low heat transfer coefficient and high thermal resistance. The thermal insulating properties of various materials are listed in Table 5.

Due to the lower thermal resistance than that of base wall, the heat transfer coefficient of the composite wall varies with the thickness of the thermal insulation material, thus affecting the heat preservation and thermal insulation of the whole building. For the aerated concrete and reinforced concrete composite wall, the heat transfer coefficient decreases with the increasing thickness of the thermal insulation material, as the calculated results shown in Figure 5. Although the thermal insulation performance can be achieved by increasing the heat preservation material, the heat transfer coefficient of the entire composite wall will remain constant when the wall thickness rises to high values. Accordingly, the external insulation of the building's external wall is constructed with an open curtain wall system in which two layers of GEPS with a thickness of 300 mm are laid in staggered joint. The fire-proof isolation belt (A-grade non-combustible fire-proof SWB) and a sealing layer of heat-insulation are set up to reduce the heat bridge generation of external wall enclosure structure. In particular, the connection mode of the invisible curtain wall keel is employed so that the connecting firmware and the joint part are all thermally insulated, leading to a heat transfer coefficient of 0.1 W/(m^2·K) for entire external wall, as the cross-section schematics show in Figure 6.

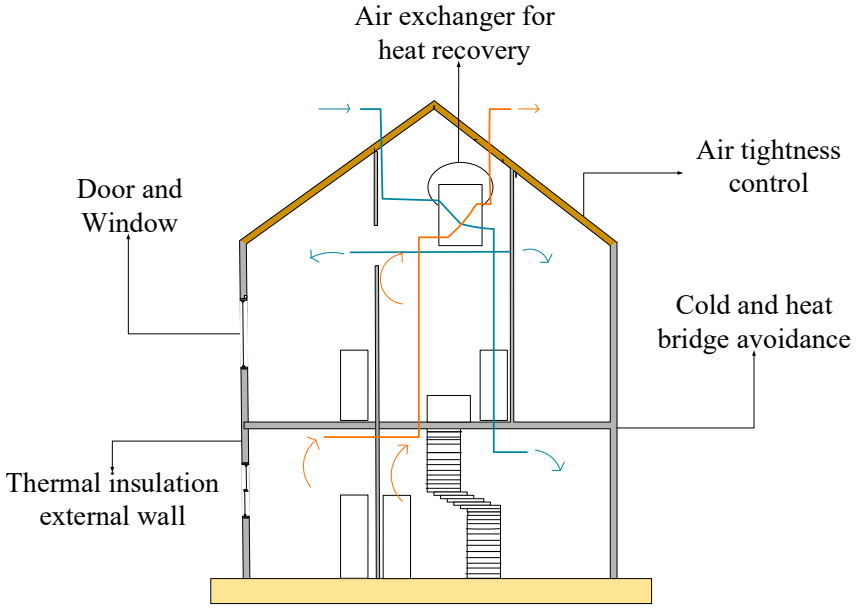

Figure 4. Schematic diagram of the passive house structure.

Table 4. Characteristics of three thermal insulation structures.

Structures	Advantages	Disadvantages
Interior insulation	1. Low requirements for insulation materials, easy to control cost; 2. Indoor construction is less dependent on environments; 3. Indoor construction is suitable for energy-saving renovation of old buildings; 4. Protecting the building facade.	1. The insulation layer inside leads to structural thermal-bridge; 2. Condensation and mildew between the insulating and structural layers; 3. Susceptible to temperature difference between day and night. 4. Difficult for secondary specialization.
Exterior insulation	1. Preventing the thermal-bridge; 2. Taking small space; 3. Extending the life space of building; 4. No requirements for wall materials; 5. Easy for secondary decoration	1. The external insulation layer has strict requirements on the fire resistance of the insulation material. 2. The construction process is increased and the quality is difficult to guarantee. 3. Easy to fall off in daily use 4. Insulation materials and structures are not comfortable.
Sandwich insulation	1. No additional requirements for insulation materials; 2. Insulation material and structure are consistent in life time; 3. Occupy small indoor space; 4. Complete construction.	1. Easy to generate thermal-bridge; 2. Complicated construction process; 3. High technical difficulty; 4. The cavity at the junction between the insulation layer and the wall affects the structural quality.

Table 5. Thermal properties of heat insulating materials.

Parameter	EPS	EFPS	PUFB	SWB
apparent density/(kg·m^{-3})	22–32	25–38	≥35	≤300
thermal conductivity/(W·m^{-1}·K^{-1})	≤0.039	≤0.035	≤0.06	≤0.04
tensile strength/MPa	≥0.1	≥0.20	≥0.15	≥0.075
dimensional stability/%	≤0.5	≤1.2	≤1.5	≤1.0
vapor permeability coefficient/(mg·Pa^{-1}·m^{-2}·s^{-1})	≤4.5	≤3.5	≤6.5	
water absorption rate/%	≤4.0	≤2.0	≤3.0	≤1.0

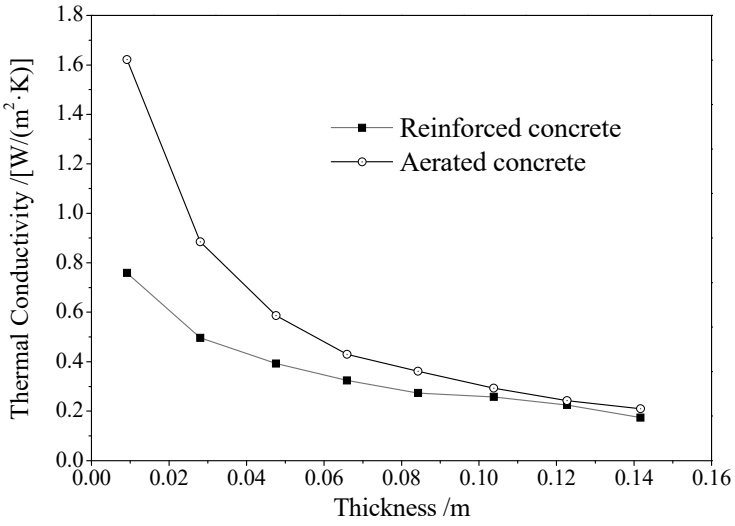

Figure 5. Heat transfer coefficients as a function of material thickness.

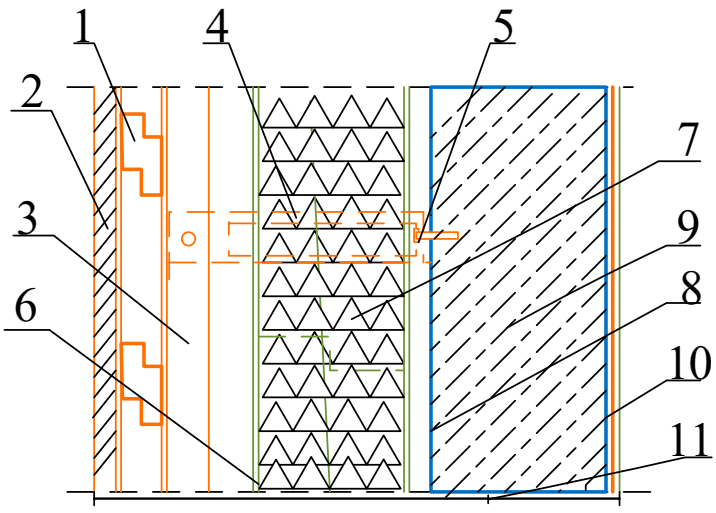

Figure 6. Schematic cross-section of external wall: (1) horizontal keel for external decoration board; (2) enhanced cement fibreboard; (3) vertical light steel keel for external decoration board; (4) thermal insulation anchorage; (5) special surface slurry; (6) composite alkali resistant glass fiber mesh cloth; (7) EPS staggered seam laying; (8) cement mortar flat layer; (9) lime mortar surface (seal layer); (10) reinforced concrete structure beam; (11) column network position axis.

3.2. Roof Insulation Structure

As a part of the non-transparent enclosure structure, building roof occupies a large area and produces serious heat loss, which dominates a majority of energy consumption. In passive buildings, the insulation layer of roof structure is specially designed thicker than that of external wall structure. Meanwhile, for maintaining an adequate humidity in room, it is necessary to add a sealing layer to the original external wall structure and lay an air-permeable waterproof layer. In order to meet the standard of ultra-low energy consumption, the external thermal insulation system comprises polymer modified surface mortar, GEPS insulation board, polymer modified surface mortar and asphalt linoleum, as shown in Figure 7 illustrating the roof thermal insulation configuration.

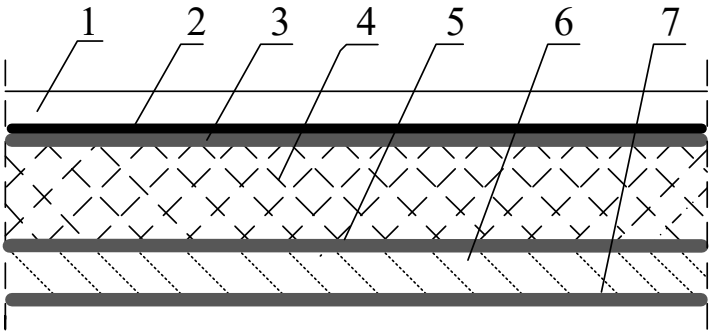

Figure 7. Thermal insulation structure of passive house roof: (1) fine stone concrete; (2) asphalt linoleum; (3) polymer plastering mortar; (4) GEPS insulation; (5) plastering mortar; (6) reinforced concrete; (7) cement plastering mortar.

3.3. Energy Conservation of Door and Window

In the whole building envelope, the house window is the weakest part with a high percentage of energy consumption approaching to 50%. Hence, improving the thermal transfer performance of window is a pivotal way to reduce the whole building's energy consumption. Senying window identified as P120, which is constituted by window frame and glass system, is the first passive window certified by German PHI in China, with the whole heat transfer coefficient being less than 0.6 W/(m^2·K). The window frame of P120 is composed of the inner aluminum-wrapped-wood frame and the outer aluminum frame which are integrated together by polymer buckle connections, as shown by the cross-sectional schematics and photograph of P120 in Figure 8. The aluminum-wrapped wood timbers are connected with Chinese traditional processes of tenon and moron to form the inner window frame, which can guarantee a moisture content of 14% and avoid the heat transfer from hardware accessories. The outer aluminum frames are welded seamlessly by patented technology to prevent joint-produced thermal bridges. The glass system is constructed in a configuration of three-glasses/two-cavities or four-glasses/three-cavities, in which the toughened low radiation glass is adopted and the air, argon, or a mixture of gas is used as thermal insulation medium.

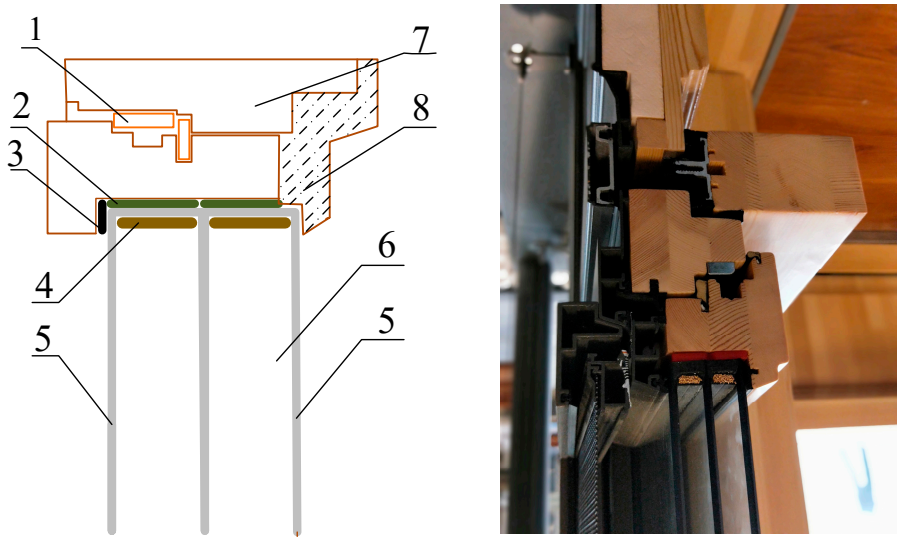

Figure 8. Window profile: (1) polymer connection clasp; (2) warm-edge interval bar; (3) seal layer; (4) dry molecular sieves; (5) tempered glass in 5 mm thickness; (6) argon in a glass cavity of 18 mm thickness; (7) window frame; (8) intensified insulation. The cross-sectional photograph of P120 window enclosure structure is also shown in the right panel.

We simulate the heat transfer of glass system by using Windows program, individually for the glass thicknesses of 12, 15, 18, and 20 mm in different window combinations, as the calculated results of thermal conductivity listed in Table 6. It is indicated that the four-glasses/three-cavities configuration represents explicitly higher performance of thermal insulation than the three-glasses/two-cavities. The heat transfer coefficient of glass system decreases with the increased thickness of argon cavity until it reaches 20 mm, while the shading coefficient (SC) and solar heat gain coefficient (SHGC) are not appreciably affected by the gas type and cavity thickness. Therefore, it is reasonably suggested that the window enclosure structure of 5GL + 15Ar + 5G + 15Ar + 5GL + 15Ar + 5GL combination can prohibit oxidization reactions of LOWE films with air and fully reduce convection and sound noise. In order to prevent joint-produced thermal bridges, the warm-edge spacers with a blending form are inserted in the connection between the glass and window frame, and the molecular sieves are used to fill internals, as shown in Figure 8 for window profile. Furthermore, the connections between window frame and the glass system are insulated with sealing tapes, and the outer side of window is intensified in insulation thickness. All these thermal insulation schemes used in passive window eventually fulfill a preferable heat transfer coefficient of <0.6 W/(m^2·K) for entire window system, as listed in Table 6.

Table 6. Heat transfer coefficients of different window combinations.

Combination	Thermal Conductivity/(W·m^{-2}·K^{-1})	SC	SHGC
5GL+12Ar+5G+12Ar+5GL	0.593	0.298	0.260
5GL+15Ar+5G+15Ar+5GL	0.565	0.299	0.260
5GL+18A+5G+18A+5GL	0.590	0.300	0.261
5GL+18Ar+5G+18Ar+5GL	0.580	0.300	0.261
5GL+18M+5G+18M+5GL	0.594	0.300	0.261
5GL+20Ar+5G+20Ar+5GL	0.590	0.300	0.261
5GL+12Ar+5G+12Ar+5GL+12Ar+5GL	0.432	0.251	0.218
5GL+15Ar+5G+15Ar+5GL+15Ar+5GL	0.377	0.251	0.218
5GL+18A+5G+18A+5GL+18A+5GL	0.472	0.250	0.217
5GL+18Ar+5G+18Ar+5GL+18Ar+5GL	0.377	0.251	0.218
5GL+18M+5G+18M+5GL+18M+5GL	0.387	0.251	0.218
5GL+20Ar+5G+20Ar+5GL+20Ar+5GL	0.385	0.249	0.216

3.4. Heat Recovery Ventilation System

The passive ultra-low energy consumption building adopts an efficient heat recovery system which combines fresh air ventilation with exhaust equipment. The high efficiency heat recovery performance of fresh air ventilation system refers to preheating or pre-cooling fresh air in the heat exchange between outdoor fresh air and indoor exhaust air to achieve the purpose of energy saving. As the schematic diagram shows in Figure 9, heat recovery mode of rotary wheel is adopted in ventilation system. In winter, the indoor return air is discharged outdoors through the upper half of a heat exchanger, by which most of the heat and moisture contained in the outdoor gas are gathered in the rotary wheel so that only the polluted air is discharged outdoors, while the outdoor fresh air introduced from the lower half of the heat exchanger is preheated and humidified by the heat and moisture accumulated in rotary wheel. Similarly, in summer, the heat recovery ventilation system can pre-cool and dehumidify outdoor air and continuously supply fresh air to the room. The complete heat recovery wheel, there is an energy-saving device to recover the energy lost in ventilation. In order to ensure the safe operation of the heat recovery system, the cryogenic medium pre-heating system is adopted in fresh air ventilation with the unit treating an air volume of 5000 m^3/h, which leads to a heat recovery efficiency more than 75%. The efficiency of heat recovery ventilation system can be calculated by the formula as follows:

$$\eta_s = 1 - \exp\left\{\frac{(mc_p)_{min}}{(mc_p)_{max}} NTU^{0.22}\left(\exp\left[-\frac{(mc_p)_{min}}{(mc_p)_{max}} NTU^{0.78}\right] - 1\right)\right\} \quad (1)$$

where η_s denotes the heat recovery efficiency, *NTU* indicates the number of heat transfer units, c_p is the fluid parameter, $(mc_p)_{min}$ represents the minimum flow rate in fresh air or exhaust air.

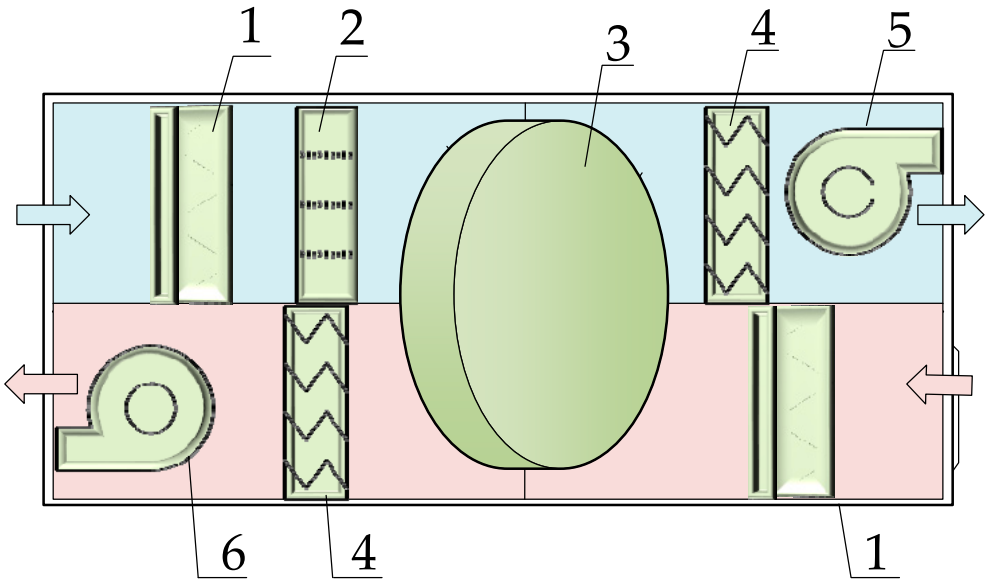

Figure 9. Schematic diagram of heat recovery ventilation system: (1) primary air filter; (2) high efficiency air filter; (3) rotary heat exchanger; (4) electrostatic precipitator; (5) air blower; (6) exhaust fan.

4. Heat Transfer and Energy Consumption Cost

4.1. Temperature and Solar Irradiation

By means of harmonic reaction method as implemented in Ecotect program, the outdoor temperature, air flow rate, and solar irradiation variation through a day are calculated to investigate the hourly thermal loads of passive building, in which the coldest and hottest days of typical weather are selected as representatives, as the results show in Figure 10. It is shown from Figure 10a that the outdoor temperature in the hottest day rises and then declines with a peak value arising at 14:00, while the coldest daily temperature fluctuates in a small magnitude with the highest and lowest values appearing at 5:00 and 13:00, respectively. As shown in Figure 10b, the hottest and coldest days represent almost identical fluctuations of air flow rate with the peak values showing at 13:00 and 14:00, respectively, although the overall air flow rate in the hottest day is distinctly lower than that in the coldest day. For the hourly solar irradiation in the hottest day, as exhibited in Figure 10c, the direct irradiation rises sharply to attain a large value at 4:00 and through a placid peak at noon and then begins to rapidly decrease at 18:00 in almost symmetrical way. The absorbed irradiation and incident irradiation peak at 10:00–12:00 with a much higher intensity than diffusive irradiation in the hottest day, while the diffusive irradiation contributes the same major part to the solar irradiation with 2 h delay of peak arising time as the absorbed irradiation and incident irradiation in the coldest day. Further for the coldest day, the direct irradiation intensity peaks at 9:00 and 12:00, with the peak value of 350 and 380 W/m^2, respectively, while the peak arising time varies similarly to the absorbed irradiation and incident irradiation.

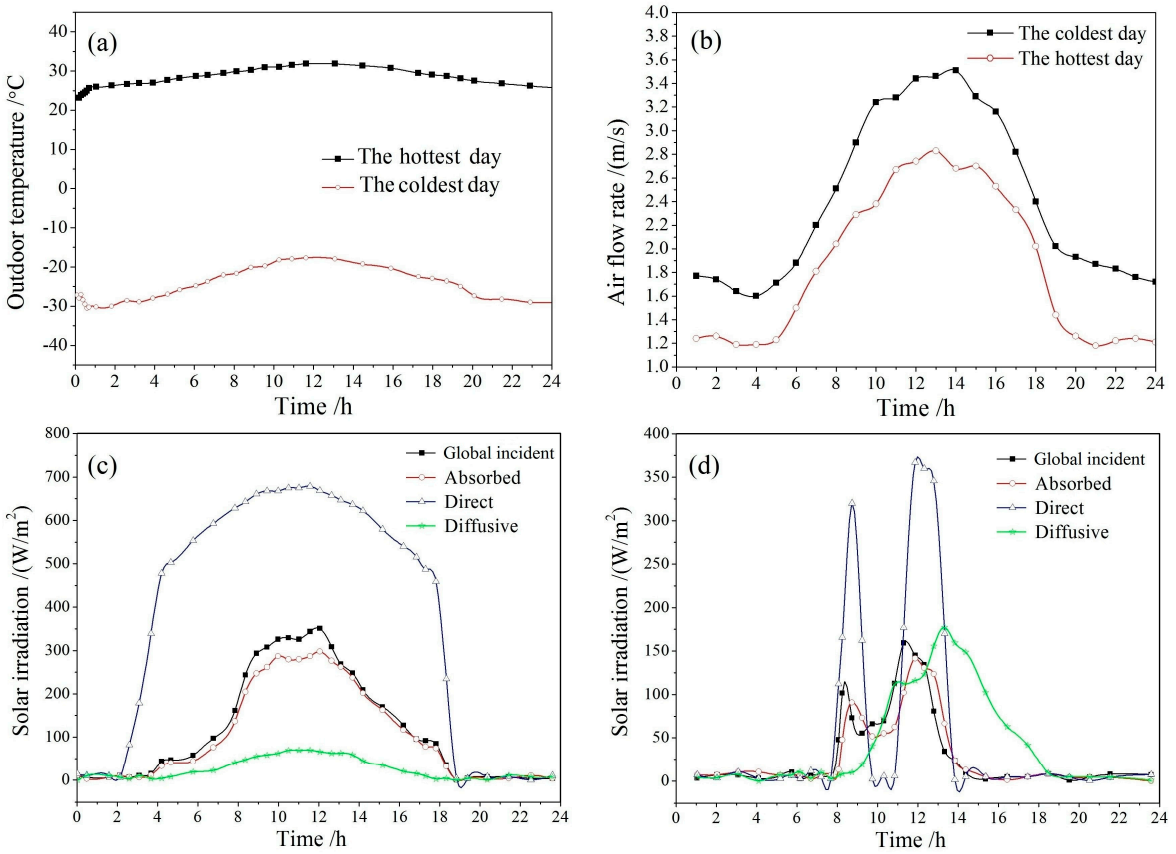

Figure 10. (**a**) Outdoor temperature and (**b**) air flow rate as a function of time; solar irradiation intensity vs. time on the (**c**) hottest day and (**d**) coldest day.

In passive building engineering, it is difficult to maintain a constant indoor temperature in severely cold area due to the greatly varying climate feature. The cooling loads in summer vary significantly through the day with the change of solar irradiation intensity, as shown in Figure 11. The total cooling load varies slightly from 0:00 to 5:00 without solar irradiation and increases intensively from 5:00 to 8:00 with the first peak of solar irradiation being reached at 8:00, after which the variation slows down until noon and then accelerates to attain the second load peak at 15:00. In comparison, the cooling load of enclosure structure is consistent with the total cooling load in summer, and the overall heating loads remain unchanged in winter. It is thus proved that the enclosure structure of passive building has acquired an excellent thermal insulation. The passive building can exploit the external enclosure structure with high thermal insulation performance to keep a constant indoor temperature, the energy consumption of which is formularized as follows:

$$Q_\tau = K \cdot F[t_z - t_n + \frac{\alpha_n}{K} \sum_1^m \frac{t_{z,n}}{\nu_n} \cos(\omega_n \tau - \psi_n - \varepsilon_n)] \quad (2)$$

where K and F denote the heat transfer coefficient and area of enclosure structure respectively, t_z symbolizes the average outdoor comprehensive temperature, t_n represents the real-time indoor comprehensive temperature, α_n indicates the heat transfer coefficient from inner surface of enclosure structure, $t_{z,n}$ and ω_n represent respectively the amplitude and frequency in n-order variation of outdoor comprehensive temperature, Ψ_n is the initial phase angle of n-order variation of outdoor comprehensive temperature, ν_n denotes the attenuation from the n-order disturbance of comprehensive temperature in enclosure structure; ν_n and ε_n respectively denote amplitude attenuation and phase delay to the

n-order disturbance of comprehensive temperature, which describe the frequency-dependent response of enclosure structure to periodic external disturbance.

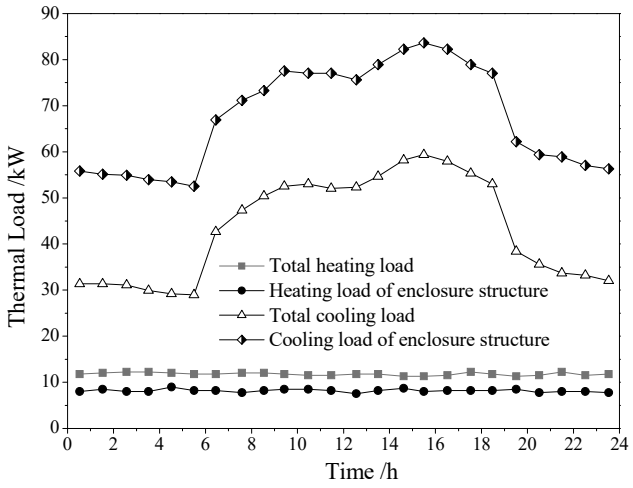

Figure 11. Thermal loads varying with time through a day in summer.

4.2. Thermal Load and Energy Demand

The three-dimensional model of passive house is established by the building information modeling method, and the harmonic response method is used to calculate the cooling and heating loads, as the simulation results listed in Table 7. In summer, the sensible cooling load of 76,759 W predominantly occupies 91% of the total cooling load of 84,154 W, while the latent and fresh air cooling loads of 7395 W and 8295 W only account for 9% and 10%, respectively. In winter, the total heating load approaches 11,450 W, which is used to compensate heat dissipation of 7622 W and 3829 W for enclosure structure and crevice permeation, respectively. The total thermal loads per unit area of 20.93 W/m^2 in summer and 2.82 W/m^2 in winter comply with the requirements of the passive building specifications. In addition, the highest thermal loads are always appearing near 14:00–15:00 whether in winter or summer.

Table 7. Simulated results of thermal load and heat dissipation.

Summer		Winter	
Cooling Load	**Results**	**Heating Load and Dissipation**	**Results**
Summer total cooling load/W	84,154	Winter total heating load/W	11,450
Peak load time/h	15:00	Peak load time/h	14:00
Sensible cooling load/W	76,759	Heat dissipation of enclosure structure/W	7622
Latent cooling load/W	7395	Heat dissipation of crevice penetration/W	3829
Fresh air cooling load/W	8265	Heating load per unit area/(W/m^2)	2.82
Cooling load per unit area/(W/m^2)	20.93		

The energy demand in passive building can be completely described by heat gain and loss of enclosure structure, the change of comprehensive temperature, the energy consumption of air penetration, the heat gain and loss of internal personnel and equipment, and the heat transfer between different local regions, as the calculated results in percentages shown in Figure 12. For cooling load, the electric power dominates energy demand in a percentage of 35.27%, while lighting and enclosure structure consume 27.13% and 20.45% of total energy, respectively, as shown in Figure 12a. For heating load, the energy demand of electric power still occupies the major part of 31.96%, which is 3.31% lower than that in cooling load, as shown in Figure 12b. In contrast to the cooling load, the 28.28% of enclosure structure is higher than the 24.58% consumed by lighting. Whether in heating or cooling

loads, the proportion of personnel energy demand is about 11%, which is smaller than that of electric power, lighting and enclosure structure, while being higher than the 2.17% and 4.07% of air penetration for cooling and heating loads, respectively.

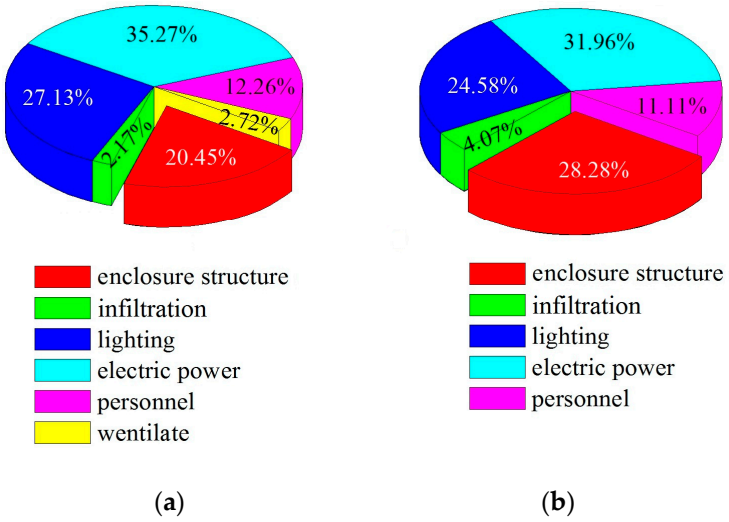

Figure 12. The energy demand percentages for (**a**) cooling load and (**b**) heating load.

The annual distribution histogram of monthly energy demand percentage in Figure 13 illustrates that the space heating accounts for more than 80% of the total energy demand from October to April of the second year, while the ventilation accounts for only about 14%. The total energy demand remarkably decreased from April to October due to the effective cooling system of natural ventilation in passive building. The energy demand of lighting, electricity, and enclosure structure accounts for the top three for both cooling and heating load through a year. Therefore, it is suggested that the EFPS be utilized for the external wall, special door, and window of passive building to improve the thermal insulation and air tightness of enclosure structure.

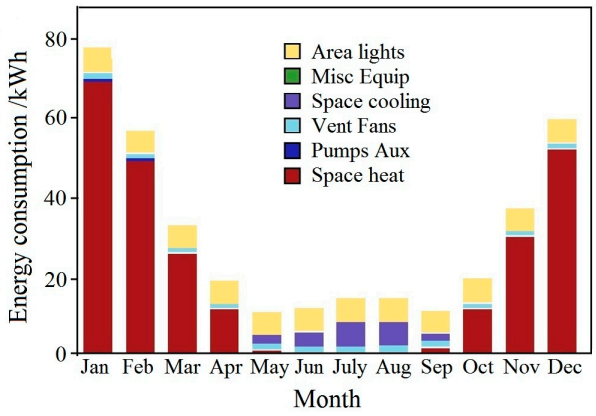

Figure 13. Total energy demand monthly through a year.

For the passive buildings with large proportion of latent heat cooling load, the energy consumption for cooling and heating of buildings is slightly different, while the energy consumption of enclosure structures still dominates the total energy consumption of buildings. In the practical project of Senying passive office building, the averaged heat transfer coefficients of external wall and window approach to 0.23 W/(m^2·K) and 1.3 W/(m^2·K), respectively, which are 50% lower than that of the external enclosure structures reported by other references [29]. Compared with other passive office buildings with similarly low energy consumption, the heating and cooling loads of Senying passive office building

are reduced by 37% and 54%, respectively, with the total energy demand being saved by 36% [30], which means Senying project completely qualifies as a high standard passive house. By adopting the insulation system of thick external wall and special doors and windows, the passive building can keep warm and avert heat dissipation in severely cold area with heavy weather to reach the purpose of deliberately reducing the building energy consumption, which can also be referenced for designing the main enclosure structure of passive building in the future.

4.3. Periodic Cost

Based on the simulation results of energy demand, the annual energy and life cycle costs and the ventilation latent heat are calculated with the cloud computing technology of Green Building Studio (GBS), as the results show in Tables 8 and 9 and Figure 14. The annual energy and life cycle costs of the passive house are 17,796 ¥, and 282,388 ¥ respectively with an annual carbon dioxide emission of 8.3 SUV, in which the annual peak energy demand of 79.9 kWh/m^2 is much less than the passive house standard of 120 kWh/m^2, as listed in Table 8. The electricity source is directly delivered from electricity power transmission center by high voltage cable; hence, there is no other exhaust emission in the energy production chain except for carbon dioxide emission. For the life cycle energy, the electric power consumption of 3638.13 kWh is higher than gasoline of 2587.96 kJ in a year. Because active mechanical cooling is not used in passive room, the energy consumption of cooling room mainly originates from natural ventilation. The natural ventilation of the modeled passive building is needed to operate for 696 h, which is only 42% of the required time for mechanical cooling, and thus can save an annual electric energy of 10,780 kWh. The energy cost analyses shown in Figure 14 imply that the space heating cost dominates the total heat energy demand (except area lighting) with an average percentage of >80% from October to April of the second year. The total energy cost reaches the highest value of 1.2 ¥/m^2 in January and attains the lowest valley of 0.3 ¥/m^2 in May and September due to the high efficiency heat transfer of natural ventilation.

Although employing energy-saving schemes in buildings will increase life cycle cost or electricity-power cost, the life cycle analyses indicate that Senying passive office building will represent 15% lower of annual energy demand than the energy consumption (676 MJ/M^2) of the other similar buildings [31] and will achieve a total annual savings of 1.8 million for heating and cooling and a total annual carbon dioxide reduction of 42 million kg in comparison to the other homologous passive buildings.

Table 8. Energy carbon cost (annual).

Energy cost/¥		17,796
Life cycle cost/¥		282,388
CO_2 emissions (large SUV equivalent)		8.3 SUV
Energy intensity/(MJ/m^2)		586
Peak energy demand/(kWh/m^2)		79.9
Life cycle energy	Electricity/kWh	3638.13
	Gasoline/kJ	2587.9

Table 9. Ventilation latent heat (annual).

Natural ventilation time/h	696
Mechanical cooling time/h	1667
Electric power saving/kWh	10,780

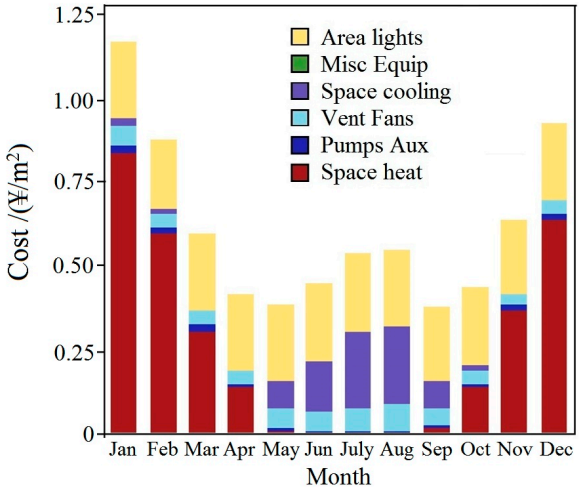

Figure 14. Total energy cost monthly through a year.

5. Conclusions

The heat transfer coefficient, cooling and heating loads, and energy demand of passive house in severely cold area are studied by heat simulations with the energy cost being analyzed to explore the widely applicable energy-saving methods. The changes of temperature and air flow rate in winter are investigated to realize preferable designs of passive building in severely cold areas, which use super thick thermal insulation structure for external wall and roof, special energy-saving window, and efficient heat recovery system. Open curtain walls are employed for the external thermal insulation system with extruded polystyrene sheets to control the heat transfer coefficient of external wall being less than 0.1 W/(m^2·K). The aluminum-coated wood window frame is combined with the four-glass/three-cavity structure to decrease heat transfer coefficient of entire window to 0.6 W/(m^2·K), in which heat-preservation interval belts are supplied to ensure sufficient air tightness. The high efficiency heat recovery system with thermal recovery rate of more than 75% can achieve a constant room temperature by recovering waste heat. The designed passive building does not need additional ground source heat pump and mechanical heating and cooling equipment in both summer and winter. The mean cooling and heating loads per area of the whole passive building are reduced to 33.58 W/m^2 and 3.79 W/m^2 respectively, with the annual energy demand decreasing to 79.9 kWh/m^2 (decreases by 33% compared with international standard), which meet and even exceed the passive specifications of buildings in Northern China.

The practical paradigm of passive building in severely cold area investigated in this paper comprises the honeycomb-type wall, the special passive doors and windows, and other super insulation enclosure structures, combining various advanced energy saving technologies of photovoltaic power generation, rainwater collection, intermediate water treatment, garbage biochemistry, and waste heat recovery. The simulation results show that it is feasible to popularize the passive office building in a severely cold area. Because of the complex factors impacting on the thermal load of passive houses, there are still some differences between the actual thermal load and energy consumption of passive houses and the simulation results from harmonic response method, which should be modified accordingly to investigate the different functional buildings with new thermal insulation materials. In the future, actual climate conditions and living habits around the world could be further combined with modern science and technology to develop more efficient HVAC systems, for example, by appropriately enlarging solar photovoltaic panels, modifying external surface colors, and optimizing geometries of roof and walls. Multi-faceted and meticulous researches are needed to further reduce building energy demand and attain the "near zero energy consumption" level in the future developments of energy-saving building and sustainable building.

Author Contributions: Conceptualization, F.W.; data curation and Formal analysis, W.-J.Y. and F.W.; investigation and writing, W.-F.S.; project administration, W.-F.S. All authors have read and agreed to the published version of the manuscript.

Funding: This research was funded by Chinese Postdoctoral Science Foundation (Grant No. 2013M531058).

Conflicts of Interest: The authors declare no conflict of interest.

References

1. Feist, W.; Schnieders, J.; Dorer, V.; Haas, A. Re-inventing air heating: Convenient and comfortable within the frame of the Passive House concept. *Energy Build.* **2005**, *37*, 1186–1203. [CrossRef]
2. Schnieders, J.; Hermelink, A. CEPHEUS results: measurements and occupants' satisfaction provide evidence for Passive Houses being an option for sustainable building. *Energy Policy* **2006**, *34*, 151–171. [CrossRef]
3. Chel, A.; Tiwari, G.N. Thermal performance and embodied energy analysis of a passive house – Case study of vault roof mud-house in India. *Appl. Energy* **2009**, *86*, 1956–1969. [CrossRef]
4. Mlakar, J.; Štrancar, J. Overheating in residential passive house: Solution strategies revealed and confirmed through data analysis and simulations. *Energy Build.* **2011**, *43*, 1443–1451. [CrossRef]
5. Kapedani, E.; Herssens, J.; Verbeeck, G. Designing for the future? Integrating energy efficiency and universal design in Belgian passive houses. *Energy Res. Soc. Sci.* **2019**, *50*, 215–223. [CrossRef]
6. Ridley, I.; Clarke, A.; Bere, J.; Altamirano, H.; Lewis, S.; Durdev, M.; Farr, A. The monitored performance of the first new London dwelling certified to the Passive House standard. *Energy Build.* **2013**, *63*, 67–78. [CrossRef]
7. Stephan, A.; Crawford, R.H.; Myttenaere, K.D. A comprehensive assessment of the life cycle energy demand of passive houses. *Appl. Energy* **2013**, *112*, 23–34. [CrossRef]
8. Stephan, A.; Crawford, R.H.; de Myttenaere, K. Multi-scale life cycle energy analysis of a low-density suburban neighbourhood in Melbourne, Australia. *Build. Environ.* **2013**, *68*, 35–49. [CrossRef]
9. Rohdin, P.; Molin, A.; Moshfegh, B. Experiences from nine passive houses in Sweden—Indoor thermal environment and energy use. *Build. Environ.* **2014**, *71*, 176–185. [CrossRef]
10. Irulegi, O.; Torres, L.; Serra, A.; Mendizabal, I.; Hernández, R. The Ekihouse: An energy self-sufficient house based on passive design strategies. *Energy Build.* **2014**, *83*, 57–69. [CrossRef]
11. Dan, D.; Tanasa, C.; Stoian, V.; Brata, S.; Stoian, D.; Nagy, G.T.; Florut, S.C. Passive house design—An efficient solution for residential buildings in Romania. *Energy Sustain. Dev.* **2016**, *32*, 99–109. [CrossRef]
12. Ilomets, S.; Kalamees, T.; Tariku, F. Indoor climate loads for dwellings in different cold climates to assess hygrothermal performance of building envelopes. *Can. J. Civ. Eng.* **2019**, *46*, 963–968. [CrossRef]
13. Fokaides, P.A.; Christoforou, E.; Ilic, M.; Papadopoulos, A. Performance of a Passive House under subtropical climatic conditions. *Energy Build.* **2016**, *133*, 14–31. [CrossRef]
14. Truong, H.; Garvie, A.M. Chifley Passive House: A Case Study in Energy Efficiency and Comfort. *Energy Procedia* **2017**, *121*, 214–221. [CrossRef]
15. Alajmi, A.; Rodríguez, S.; Sailor, D. Transforming a passive house into a net-zero energy house: a case study in the Pacific Northwest of the U.S. *Energy Conv. Manag.* **2018**, *172*, 39–49. [CrossRef]
16. Yu, Z.; Gou, Z.; Qian, F.; Fu, J.; Tao, Y. Towards an optimized zero energy solar house: A critical analysis of passive and active design strategies used in Solar Decathlon Europe in Madrid. *J. Clean. Prod.* **2019**, *236*, 117646. [CrossRef]
17. Dalbem, R.; Grala da Cunha, E.; Vicente, R.; Figueiredo, A.; Oliveira, R.; da Silva, A.C.S.B. Optimisation of a social housing for south of Brazil: From basic performance standard to passive house concept. *Energy* **2019**, *167*, 1278–1296. [CrossRef]
18. Wang, Y.; Du, J.; Kuckelkorn, J.M.; Kirschbaum, A.; Gu, X.; Li, D. Identifying the feasibility of establishing a passive house school in central Europe: An energy performance and carbon emissions monitoring study in Germany. *Renew. Sustain. Energy Rev.* **2019**, *113*, 109256. [CrossRef]
19. Zhang, S.H.; Zhuang, Z.; Hu, Y.D.; Yang, B.S.; Tan, H.W. Applicability Study on a Hybrid Renewable Energy System for Net-Zero Energy House in Shanghai. *Energy Procedia* **2016**, *88*, 768–774. [CrossRef]
20. Chen, X.; Yang, H.X. Integrated energy performance optimization of a passively designed high-rise residential building in different climatic zones of China. *Appl. Energy* **2018**, *215*, 145–158. [CrossRef]

21. Li, R.; Wang, M.; Zhu, J. Indoor Thermal Environment Monitoring and Evaluation of Double-Deck Prefabricated House in Central China—Taking Zhengzhou Area as an Example. *Energy Procedia* **2019**, *158*, 2812–2819. [CrossRef]
22. Li, C.; Zhou, D.Q.; Wang, H.; Cheng, H.B.; Li, D.D. Feasibility assessment of a hybrid PV/diesel/battery power system for a housing estate in the severe cold zone—A case study of Harbin, China. *Energy* **2019**, *185*, 671–681. [CrossRef]
23. Liu, J.Z.; Zhou, Q.X.; Tian, Z.Y.; He, B.J.; Jin, G.Y. A comprehensive analysis on definitions, development, and policies of nearly zero energy buildings in China. *Renew. Sust. Energ. Rev.* **2019**, *114*, 109314. [CrossRef]
24. Liu, J.Z.; Liu, Y.W.; He, B.J.; Xu, W.; Jin, G.Y.; Zhang, X.T. Application and suitability analysis of the key technologies in nearly zero energy buildings in China. *Renew. Sust. Energ. Rev.* **2019**, *101*, 329–345. [CrossRef]
25. Yang, L.; He, B.J.; Ye, M. Application research of Ecotect in residential estate planning. *Energy Build.* **2014**, *72*, 195–202. [CrossRef]
26. He, X.; Kong, Q.; Xiao, Z. Fast simulation methods for dynamic heat transfer though building envelope based on model-order-reduction. *Procedia Eng.* **2015**, *121*, 1764–1771. [CrossRef]
27. Yao, R.; Costanzo, V.; Li, X.; Zhang, Q.; Li, B. The effect of passive measures on thermal comfort and energy conservation. A case study of the hot summer and cold winter climate in the Yangtze River region. *J. Build. Eng.* **2018**, *15*, 298–310. [CrossRef]
28. Li, N.; Chen, Q. Experimental study on Heat Transfer Characteristics of Interior Walls under Partial-Space Heating Mode in Hot Summer and Cold Winter Zone in China. *Appl. Therm. Eng.* **2019**, *162*, 114264. [CrossRef]
29. Ballarini, I.; De Luca, G.; Paragamyan, A.; Pellegrino, A.; Corrado, V. Transformation of an office building into a nearly zero energy building (nZEB): Implications for thermal and visual comfort and energy performance. *Energies* **2019**, *12*, 895. [CrossRef]
30. Szymon, F. Cost-optimal plus energy building in a cold climate. *Energies* **2019**, *12*, 3841. [CrossRef]
31. Gustafsson, M.S.; Myhren, J.A.; Dotzauer, E.; Gustafsson, M. Life cycle cost of building energy renovation measures, considering future energy production scenarios. *Energies* **2019**, *12*, 2719. [CrossRef]